

THERMAL AND SPECTROSCOPIC CHARACTERIZATION OF SEVERAL DERIVATIVES CONTAINING A NEW ORGANIC RING SYSTEM The tropane-6-spiro-5'-hydantoin structure

P. J. Sánchez-Soto^{a}, M. Villacampa^b, J. M. Ginés^c,
A. Ruiz-Conde^a, M. A. Avilés^a and M. J. Arias^c*

^aInstituto de Ciencia de Materiales, Centro Mixto Consejo Superior de Investigaciones Científicas (C.S.I.C.)-Universidad de Sevilla, c/Américo Vespucio s/n, Isla de La Cartuja 41092-Sevilla

^bDepartamento de Química Orgánica y Farmaceútica, Facultad de Farmacia, Universidad Complutense, 28040-Madrid

^cDepartamento de Farmacia y Tecnología Farmacéutica, Facultad de Farmacia, Universidad de Sevilla, c/Professor García González s/n, 41012-Sevilla, Spain

(Received January 31, 1997)

Abstract

Several derivatives containing a new organic ring system, the tropane-6-spiro-5'-hydantoin structure (namely 8-alkyl-8-azabicyclo [3.2.1.] octane-6-spiro-5'-imidazoline-2',4'-diones) have been characterized by thermal (DSC and simultaneous DTA-TG-DTG) and spectroscopic techniques (IR, ¹H-NMR, ¹³C-NMR). X-ray powder diffraction and elemental analysis were applied for structural and molecular characterization. All the compounds melt in the range 160–250°C and undergo decomposition with progressive mass loss after the solid-liquid thermal transition with molecular degradation. It was found that tropane-6-spiro-5'-hydantoin derivatives with the hydantoin ring in β position are thermally less stable than those containing this ring in α position.

Keywords: DTA, DSC, hydantion, new ring, tropane, X-ray

Introduction

Urea and some of its derivatives have already been extensively studied by combined thermal methods [1–6]. However, cyclic derivatives of urea containing carbonyl groups, as barbiturates and hydantoins, have scarcely been studied [2, 7]

* Author to whom all correspondence should be addressed.

The synthesis of tropane and nortropane-3-spirohydantoins has been described in previous papers [8–14]. In particular, several tropane and nortropane-3-spiro-5'-hydantoins have shown interesting and good pharmacological properties as anticholinergic, analgesic, anticonvulsant, antiarrhythmic and antiinflammatory agents [12, 13]. The activity of some derivatives as antiinflammatory agents was found superior to that of phenylbutazone and comparable to that of indometacine. To achieve efficient antiinflammatory agents devoid of the central nervous system depressant activity led to design and preparation of more polar derivatives in order to avoid passage through the blood-brain barrier. According to these premises, the synthesis and stereochemistry of hydroxy- and dihydroxy-derivatives containing the tropane-3-spiro-5'-hydantoin ring have been reported recently [15–17]. The synthesis of their positional isomers containing a new ring system, namely the tropane-6-spiro-5'-hydantoin structure was also considered of interest.

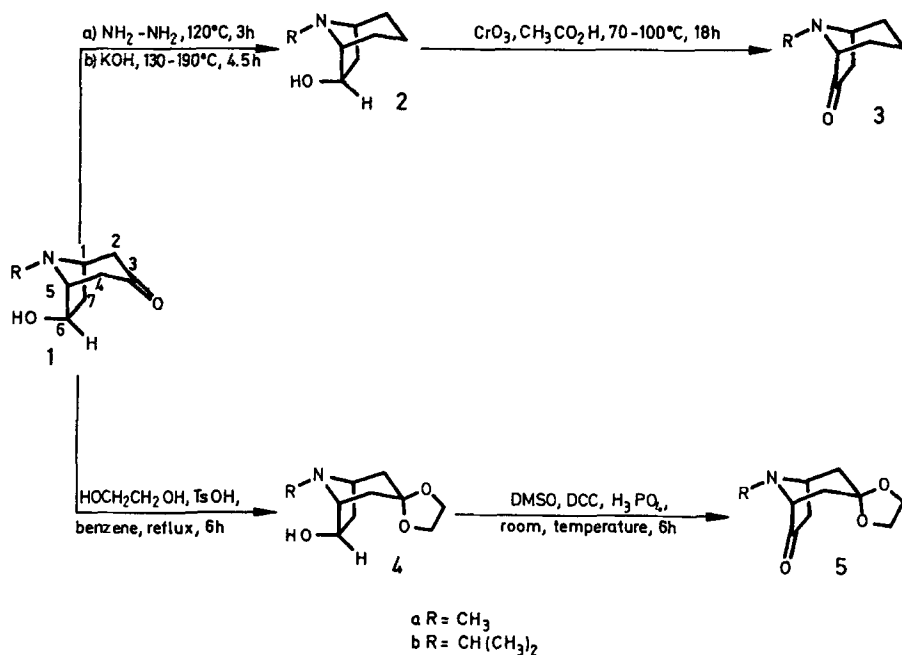
In the present work, a thermal (using simultaneous DTA-TG-DTG and DSC) and spectroscopic study (using IR, $^1\text{H-NMR}$ and $^{13}\text{C-NMR}$) of several derivatives containing this new ring system is reported. X-ray powder diffraction methods and elemental analysis were also applied for structural and molecular characterization.

Experimental

Materials

The synthesis of derivatives containing the tropane-6-spiro-5'-hydantoin ring has been performed according to procedures described previously for the preparation of their positional isomers [14–16]. All the chemicals were employed as received from commercial suppliers (Aldrich, Fluka, Merck, Carlo Erba, Scharlau, Probus and Panreac). Schemes 1 and 2 show the main general features. Compounds 1a, 2a and 3b were prepared according to the method proposed by Dewar *et al.* [11] with minor modifications, and compounds 4a and 5a were prepared according to the method described by Montza and Matiskella [18]. Compounds 1a and 1b were reduced under Wolff-Kirshner conditions to derivatives 2a and 2b. Oxidation of 2 with two equivalents of chromium (VI) oxide in acetic acid at 70–100°C for 16 h led to the desired tropan-6-ones 3a and 3b. Preparation of 3-oxohydantoins 7 and 8 depicted in scheme 2 required the previous synthesis of ketones 5, which was achieved by protection of the carbonyl group of 1a,b with 1,2-ethanediol to yield 4 and 4b (scheme 1), followed by dimethylsulfoxide (DMSO)-dicyclohexyl carbodiimide (DCC) oxidation [19] to the corresponding ketones 5a and 5b, as shown in Scheme 1.

Preparation of compounds 8 through Bucherer-Bergs reaction of diketone 6 was unsuccessfully attempted, being prepared by acid hydrolysis of 5. Compound 6 presented a low stability and the crude hydrolysis product treated under

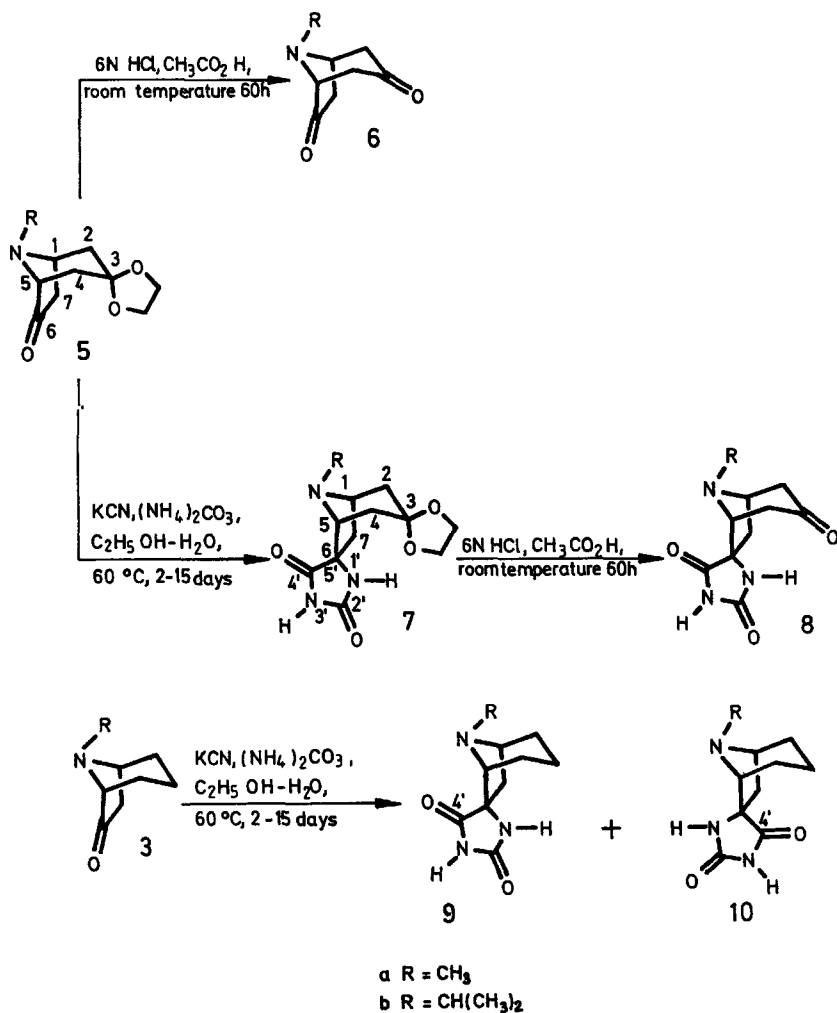


Scheme 1

Bucherer-Bergs conditions yielded a complex mixture. An alternative route (see Scheme 2) was devised, where Bucherer-Bergs reactions of compounds 5 to give hydantoin 7, followed by deprotection of the carbonyl group at C₃ gave the desired compound 8. This kind of reaction was found stereoselective [15–17], thus yielding the isomer with an *exo*-orientation for C₄, as unique product.

An attempt to prepare the tropane-3,6-bis-spirohydantoin system by Bucherer-Berg reaction of compounds 8 led only to recovery of the starting material. Previous efforts by other authors [20] to transform diketones into dihydantoin were unsuccessful, and monohydantoin were the only isolated products. This fact was attributed to precipitation of the compounds from the reaction medium. However, it was found that compounds 8 were readily soluble in the 1:1 ethanol-water mixture employed in the synthesis [15] and therefore the failure of the reaction must be due to steric hindrance on C₃ to axial attack of cyanide, due to the presence of the hydantoin ring in C₆.

On the other hand, Bucherer-Bergs reaction of ketones 3 (Scheme 2) yielded a 9:1 mixture of the hydantoin 9a and 10a and a 5.5:1 mixture of 9b and 10b, in contrast with the behaviour observed previously for tropane-3-ones [21], which afforded exclusively the product with an equatorial stereochemistry for the C₄, atom of the hydantoin system. Compounds with hydantoin ring as found in 9 are designated β , and designated α as found in 10 (Scheme 2).



Scheme 2

According to the above synthetic methods, only the compounds that were purified are studied here.

Methods

Infrared spectra (IR) were recorded on a Nicolet FTIR spectrometer model 510 using KBr compressed pellets.

¹H Nuclear Magnetic Resonance (1H-NMR) spectra were obtained on the following instruments: Hitachi Perkin-Elmer R-24B (60 MHz) and Varian VXR-

300 (300 MHz). The ^{13}C Nuclear Magnetic Resonance (^{13}C -NMR) spectra (75.4 MHz) were measured with the latter instrument. Deuteriochloroform or DMSO- d_6 were used as solvents, and tetramethylsilane (TMS) was added in all cases as internal standard. All chemical shifts are referred to TMS and are given in the delta scale and all J values are given in Hz. Only the J values that could be measured accurately are given.

Elemental analysis were performed on a Carlo-Erba 1104 CHN microanalyzer.

Melting points were measured in open capillary glass tubes using a Büchi immersion apparatus and are subjective estimates.

X-ray powder diffraction diagrams (XRD) were obtained in random oriented samples using a Siemens D-501 equipment. Ni-filtered $\text{CuK}\alpha$ radiation and graphite monochromator, scanning from 2 to 70 ($^\circ 2\theta$).

Differential Scanning Calorimetry (DSC) runs were obtained in a Mettler DSC equipment, model FP85, by heating from room temperature to 360 $^\circ\text{C}$ at 10 $^\circ\text{C min}^{-1}$. Finely powdered samples were exactly weighed and encapsulated in flat-bottomed aluminium pans of 45 μl volume with crimped-on lids. Heats of fusion were determined following calibration with indium (28.4 $\text{J}\times\text{g}^{-1}$) using integration of the areas under the DSC endothermal peaks.

DTA and TG curves were recorded simultaneously in nitrogen flow using a high-temperature thermal analyzer Setaram 92, model 16–18 at a heating rate of 10 $^\circ\text{C min}^{-1}$. Samples were gently packed into open Pt crucibles and thermally treated from room temperature (20 $^\circ\text{C}$) up to 1000 $^\circ\text{C}$.

Results and discussion

Selected compounds containing the new organic ring system tropane-6-spiro-5'-hydantoin synthesized according to Scheme 2 have been characterized by IR, ^1H -NMR and ^{13}C -NMR spectroscopy methods and elemental analysis (C, H, N). Only the data for compounds that were purified are reported here. The NMR results of selected derivatives are listed in Tables 1 and 2. The IR spectra of compounds 7b, 9b and 10b are shown in Fig. 1. The results obtained by these techniques can be summarized as follows:

Compound 7a: (\pm)-(1R*, 5S*, 6R*)-3,3-Ethylenedioxy-8-methyl-8-azabicyclo[3.2.1]octane-6-spiro-5'-imidazolidine-2',4'-dione. Yield, 66%, after 7 days or reaction and crystallization from ethyl acetate. Anal. calcd. for $\text{C}_{12}\text{H}_{17}\text{N}_3\text{O}_4$: C, 53.92; H, 6.41; N, 15.72. Found: C, 54.09; H, 6.61; N, 15.60% IR (KBr): 3420 (N-H), 1780, 1730 (C=O) cm^{-1} .

Compound 7b: (\pm)-(1R*, 5S*, 6R*)-3,3-Ethylenedioxy-8-isopropyl-8-azabicyclo[3.2.1]octane-6-spiro-5'-imidazolidine-2',4'-dione. Yield, 62%, after 7 days or reaction and crystallization from ethanol. Anal. calcd. for $\text{C}_{14}\text{H}_{21}\text{N}_3\text{O}_4$: C, 56.93; H, 7.16; N, 14.22. Found: C, 57.05; H, 7.38; N, 14.17% IR (KBr): 3384 (N-H), 1777, 1717 (C=O) cm^{-1} .

Table 1a $^1\text{H-NMR}$ spectra of compounds 7a, 7b, 9b and 10b (300 MHz, CDCl_3)

Compound	$\text{N}_{1/}$ -H	$\text{N}_{3/}$ -H	C_1 -H	C_5 -H	C_7 -H ^{exo}	C_7 -H ^{endo}	C_3 -H _{ax}	C_3 -H _{eq}
7a ^x	6.60(s)	10.50(s)	3.24(m)	3.21(m)	2.38(dd)	1.92(d)	-	-
7b	6.79(s)	8.33(s)	3.66(m)	3.58(m)	2.59(dd)	2.06(d)	-	-
9b	6.08(s)	7.69(s)	3.57(m)	3.45(s)	2.71(dd)	1.75(m)	1.76(m)	1.20(m)
10b	6.04(s)	8.25(s)	3.57(m)	3.24(s)	2.30(dd)	2.43(d)	2.37(m)	1.09(m)

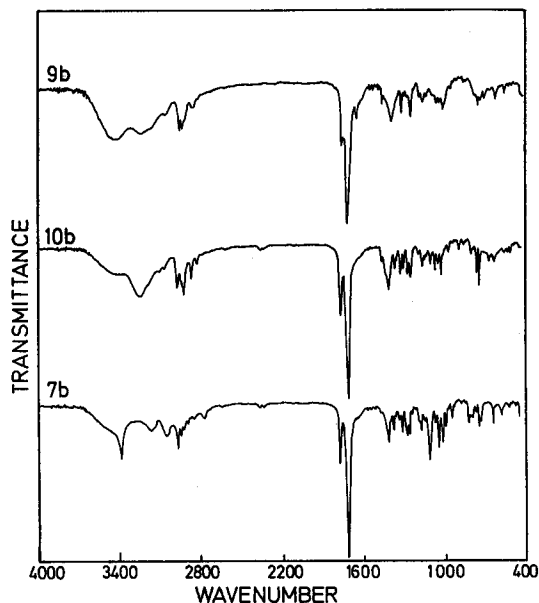
Table 1 Continued

Compound	$C_{(2)A}-H_{ax}$	$C_{(2)A}-H_{ax}$	R^{**}	OCH_2-CH_2O
7a ^x	2.08(dd, $J=14.1$ and 3.0)	1.76(d)	2.37(s)	4.06-3.62
7b	2.02(dd, $J=14.8$ and 4.0)	1.59(d)	3.02(m)	(m,4H)
	2.21(dd, $J=14.4$ and 3.2)	1.60(d)		4.08-3.91
9b	2.09(dd, $J=15.1$ and 4.2)	1.81(d)	1.11(d)	(m,4H)
			1.07(d)	
10b		1.50(m)	3.17(m)	
			1.09(d)	
		1.91(m)	1.05(d)	
	1.78(m)	1.54(m)	3.19(m)	
		1.38(m)	1.06,1.03(2d)	

^xDMSO-*d*₆ $J_{1,7exo}=7.0$ and $J_{gem}=13.0$ Hz $J=6.1$ Hz

Table 2 ^{13}C -NMR data for compounds 9b and 10b (75.4 MHz, $\text{DMSO}-d_6$)

Position	Compound 9b		Compound 10b	
	δ/ppm	$^1J(^{13}\text{C}-\text{H})/\text{Hz}$	δ/ppm	$^1J(^{13}\text{C}-\text{H})/\text{Hz}$
C ₁	53.45(d)	141.7	52.78 (d)	142.6
C ₂	22.12 (t)	125.4	20.90 (t)	125.2
C ₃	15.87 (t)	126.4	15.62 (t)	126.4
C ₄	17.45 (t)	125.8	17.44 (t)	125.3
C ₅	60.33 (d)	143.0	65.05 (d)	143.11
C ₆	67.20 (s)	—	69.54 (s)	—
C ₇	38.92 (t)	132.1	40.81 (t)	132.7
C _{2'}	157.48	4.4*	156.27	—
C _{4'}	178.81	16.0*	176.33	7.4*
R	43.63 (d, CH)	130.4	43.22 (d, CH)	130.4
	21.17 (q, CH ₃)	125.4	21.35 (q, CH ₃)	125.4
	21.92 (q, CH ₃)	125.4	21.99 (q, CH ₃)	125.4

**Fig. 1** FTIR spectra of compounds 7b, 9b and 10b

Compound 9a: (\pm)-(1S*, 5R*, 6R*)-8-methyl-8-azabicyclo[3.2.1]octane-6-spiro-5'-imidazolidine-2',4'-dione and Compound 10a (\pm)-(1S*, 5R*, 6S*)-8-methyl-8-azabicyclo[3.2.1]octane-6-spiro-5'-imidazolidine-2',4'-dione Yield,

30% (9a:10a=9.1 by $^1\text{H-NMR}$), after 15 days of reaction and column chromatography (silica gel), eluting with 9:1 chloroform-ethanol. An analytical sample of 9a was obtained by recrystallization from ethanol. Compound 10a could not be purified. Data for compound 9a: Anal. Calcd. for $\text{C}_{10}\text{H}_{15}\text{N}_3\text{O}_4$: C, 57.40; H, 7.22; N, 20.08. Found: C, 57.30; H, 7.42; N, 20.04% IR (KBr): 3420, 3320 (N-H), 1770, 1730 (C=O) cm^{-1} .

Compound 9b: (\pm)-(1S*, 5R*, 6R*)-8-isopropyl-8-azabicyclo[3.2.1]octane-6-spiro-5'-imidazolidine-2',4'-dione. Yield, 28%, after 2 days of reaction and separation from 10b by column chromatography (alumina), eluting with 95:5 chloroform-ethanol. Anal. calcd. for $\text{C}_{12}\text{H}_{19}\text{N}_3\text{O}_2$: C, 60.73; H, 8.06; N, 17.70. Found: C, 60.49; H, 7.98; N, 17.63% IR (KBr): 3280–3160 (N-H), 1775, 1722 (C=O) cm^{-1} .

Compound 10b: (\pm)-(1S*, 5R*, 6S*)-8-isopropyl-8-azabicyclo[3.2.1]octane-6-spiro-5'-imidazolidine-2',4'-dione. Yield, 5%, after 2 days of reaction and separation from 9b by column chromatography (alumina), eluting with 95:5

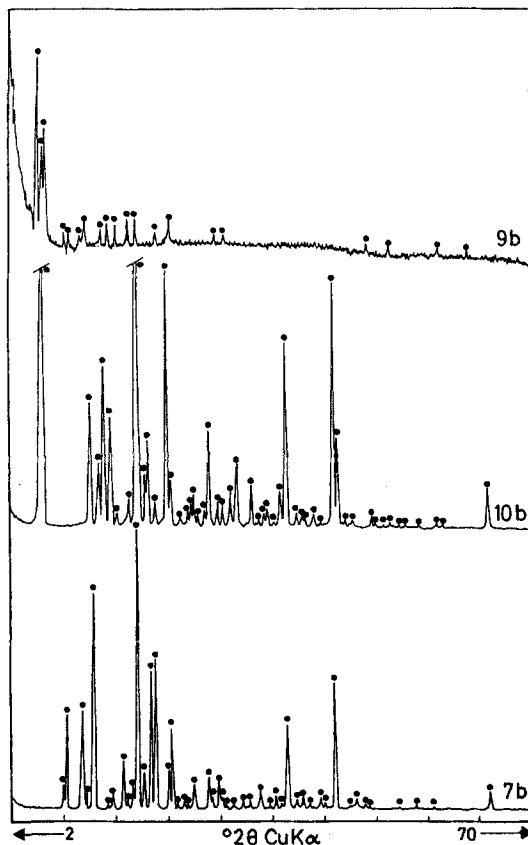


Fig. 2 XRD diagrams of compounds 7b, 9b and 10b

chloroform:ethanol. Anal. calcd. for $C_{12}H_{19}N_3O_2$: C, 60.73; H, 8.06; N, 17.70. Found: C, 60.33; H, 8.00; N, 17.59%. IR (KBr): 3280–3160 (N–H), 1775, 1727 (C=O) cm^{-1} .

The main stereochemical features of compounds designated 7–10 have been established taking into account 1H -NMR and ^{13}C -NMR data [15–17]. They are, in summary, the stereochemistry of the N-alkyl chain and of the spiro atom, together with the conformation of the piperidine moiety. Thus, the ^{13}C -NMR chemical shift values (Table 2) for C_2 and C_4 are attributed to an axial orientation of the N-alkyl chain. The exo-stereochemistry for $C_{4'=O}$ groups must be attributed to compounds 9, thus supporting the structures depicted in Scheme 2. The stereochemistry found for the major product of the Bucherer-Bergs reaction is consistent with the results described by Tager and Christensen for norbornene [22].

Table 3 X-ray data of compound 7b: (\pm)-(1R*, 5S*, 6R*)-3,3-ethylenedioxy-8-isopropyl-8-azabicyclo [3.2.1] octane-6-spiro-5'-imidazolidine-2',4'-dione. (Seq=peaks Sequence as shown Fig. 2; Ni filtered CuK_{α} radiation $^{\circ}2\theta$; $d(\text{\AA})$ = interlayer distances in \AA ; III_o = relative intensities). 1 \AA = 0.1 nm

Seq	$^{\circ}2\theta$	$d/\text{\AA}$	III_o
1	8.700	10.1557	9
2	9.126	9.6821	34
3	11.268	7.8464	35
4	11.700	7.5576	4
5	12.751	6.9369	76
6	14.439	6.1295	2
7	15.142	5.8467	6
8	16.544	5.3541	17
9	16.950	5.2267	4
10	17.759	4.9905	8
11	18.365	4.8272	100
12	19.202	4.6185	13
13	20.127	4.4083	49
14	20.765	4.2742	53
15	22.450	3.9571	15
16	22.856	3.8878	28
17	23.546	3.7754	2
18	24.476	3.6340	3
19	24.941	3.5673	2
20	25.761	3.4556	9

Table 3 Continued

Seq	$^{\circ}2\Theta$	$d/\text{Å}$	III_0
21	27.775	3.2093	12
22	28.150	3.1675	4
23	29.129	3.0632	10
24	29.550	3.0205	4
25	29.964	2.9797	3
26	30.900	2.8915	2
27	31.049	2.8780	2
28	32.256	2.7730	3
29	33.180	2.6979	3
30	34.559	2.5933	7
31	35.730	2.5110	2
32	36.575	2.4549	5
33	37.352	2.4056	2
34	38.090	2.3606	30
35	39.334	2.2888	4
36	40.100	2.2468	5
37	40.950	2.2021	2
38	42.349	2.1326	5
39	42.883	2.1073	3
40	44.278	2.0440	45
41	46.279	1.9602	2
42	47.150	1.9260	4
43	48.217	1.8859	2
44	48.815	1.8641	2
45	52.706	1.7353	1
46	54.868	1.6719	2
47	57.190	1.6094	1
48	64.504	1.4435	7

$^1\text{H-NMR}$ results also support the proposed structures (Table 1). Thus, comparison of the $^1\text{H-NMR}$ spectra of compounds 9b and 10b shows an upfield shift of 0.6 ppm for the $\text{C}_3\text{-H}_{\text{ax}}$ proton of 10b with respect to the corresponding atom

of 9b, attributed to the anisotropic effect of the $C_{4'}=O$ group. When N_1 , occupies the *exo* position (compounds 10), it exerts similar effects on C_7-H_{exo} and C_7-H_{endo} , and the chemical shifts of these protons are very similar. In compounds 9, instead, the C_6-N_1 , bonds is *syn* with respect to the C_7-H_{endo} bond, and *anti* with respect to the C_7-H_{exo} bond; this explains the fact that the chemical shifts of these protons differ by ca. 1 ppm, providing additional evidence in favour of the structures 9b and 10b.

Chemical shift values of C_2 and C_4 (Table 2) are in accordance with a conformation of the piperidine ring as a flattened chair. These values would be displaced to higher fields in boat structures [8]. In fact, coupling constants $J_{1,2ax}$ and

Table 4 X-ray data of compound 9b: (\pm)-(1S*, 5R*, 6R*)-8-isopropyl-8-azabicyclo [3.2.1] octane-6-spiro-5'-imidazolidine-2',4'-dione. (Seq = peaks Sequence as shown Fig. 2; Ni filtered CuK_{α} radiation $^{\circ}2\Theta$; $d(\text{\AA})$ = interlayer distances in \AA ; III_0 = relative intensities). $1 \text{\AA} = 0.1 \text{ nm}$

Seq	$^{\circ}2\Theta$	$d/\text{\AA}$	III_0
1	5.673	15.5663	100
2	6.387	13.8282	61
3	6.700	13.1821	69
4	9.152	9.6548	26
5	9.900	8.9277	26
6	11.287	7.8330	24
7	11.931	7.4118	30
8	14.063	6.2926	37
9	14.700	6.0213	42
10	15.900	5.5694	39
11	17.400	5.0925	51
12	18.333	4.8355	51
13	19.827	4.4742	49
14	21.108	4.2055	57
15	22.816	3.8944	67
16	28.901	3.0868	53
17	30.075	2.9689	50
18	48.811	1.8643	23
19	51.639	1.7686	22
20	58.044	1.5878	20
21	62.032	1.4949	21

$J_{4ax,5}$, had values of 3–6 Hz in those compounds where they could be accurately measured (compound 7), and were different from $J_{1,2eq}$ and $J_{4eq,5}$, each <1 Hz. Therefore, the dihedral angle $H_{2,4eq}-C-C-H_{1,5}$ is larger than $H_{2,4ax}-C-C-H_{1,5}$, and thus the chair must be flattened.

Table 5 X-ray data of compound 10b: (\pm)-(1S*, 5R*, 6S*)-8-isopropyl-8-azabicyclo [3.2.1] octane-6-spiro-5'-imidazolidine-2',4'-dione. (Seq = peaks Sequence as shown Fig. 2; Ni filtered CuK_{α} radiation $^{\circ}2\Theta$; $d(\text{\AA})$ = interlayer distances in \AA ; III_o = relative intensities). $1 \text{\AA} = 0.1 \text{ nm}$

Seq	$^{\circ}2\Theta$	$d/\text{\AA}$	III_o
1	6.269	14.0880	100
2	12.471	7.0918	9
3	13.550	6.5296	5
4	14.215	6.2257	11
5	15.147	5.8446	8
6	15.882	5.5757	1
7	17.399	5.0928	2
8	18.492	4.7942	25
9	19.550	4.5371	4
10	19.896	4.4589	6
11	20.805	4.2661	2
12	22.361	3.9727	18
13	22.829	3.8923	4
14	24.099	3.6900	<1
15	25.164	3.5362	1
16	25.551	3.4835	2
17	25.935	3.4327	2
18	26.486	3.3626	1
19	27.406	3.2517	1
20	27.917	3.1933	7
21	29.065	3.0698	2
22	29.798	2.9960	2
23	30.827	2.8983	3
24	31.626	2.8268	5
25	33.545	2.6693	3

Table 5 Continued

Seq	$^{\circ}2\Theta$	$d/\text{\AA}$	I/I_0
26	34.473	2.5996	<1
27	35.239	2.5448	1
28	35.655	2.5161	1
29	36.515	2.4588	<1
30	37.408	2.4021	3
31	38.097	2.3602	13
32	39.522	2.2784	1
33	40.283	2.2371	1
34	40.500	2.2255	1
35	41.764	2.1610	1
36	42.651	2.1182	<1
37	44.294	2.0433	17
38	44.800	2.0214	6
39	45.829	1.9784	<1
40	46.867	1.9370	<1
41	49.304	1.8468	1
42	49.777	1.8303	<1
43	50.887	1.7930	<1
44	51.693	1.7669	<1
45	52.940	1.7282	<1
46	53.747	1.7041	<1
47	55.513	1.6540	<1
48	57.802	1.5938	<1
49	58.661	1.5725	<1
50	64.507	1.4434	3

X-ray powder diffraction diagrams corresponding to these derivatives are shown in Fig. 2, showing that they are all crystallized compounds, although no single crystals suitable for X-ray structural determination have been obtained. Attempts to prepare them have been unsuccessful up to now and, consequently, the crystallographic constants and space groups are not available. Tables 3, 4 and 5 report interlayer distances and relative X-ray intensities for these compounds

using $\text{CuK}\alpha$ radiation, including selected peaks as labelled in Fig. 2. Sample 9 shows the maximum interlayer distance at 15.56 Å (Table 4), this value being the maximum for the group. Differences in X-ray diffraction patterns of samples 9b and 10b are ascribed to structural differences in stereochemistry, as deduced from spectroscopic data included in Tables 1 and 2 discussed above.

Figure 3 shows the DSC curves of compounds 9b, 10b and 7b. Table 6 summarizes the DSC results including onset and peak melting temperatures, melting enthalpies and melting temperatures estimated using an open glass capillary tube and the Büchi immersion apparatus. All the samples investigated melt in the range 150–250°C, depending on the structural features (Scheme 2). Compound 10b melts at lower temperature than its stereoisomer 9b, which may be attributed to molecular group associations. In fact, compound 7b melts at slightly lower temperature than 10b despite the fact that the first one has a higher molecular weight and an additional $-\text{O}-\text{CH}_2-\text{CH}_2-\text{O}-$ substituent. Sample 7b, being the sample with the highest molecular weight shows the highest value of melting

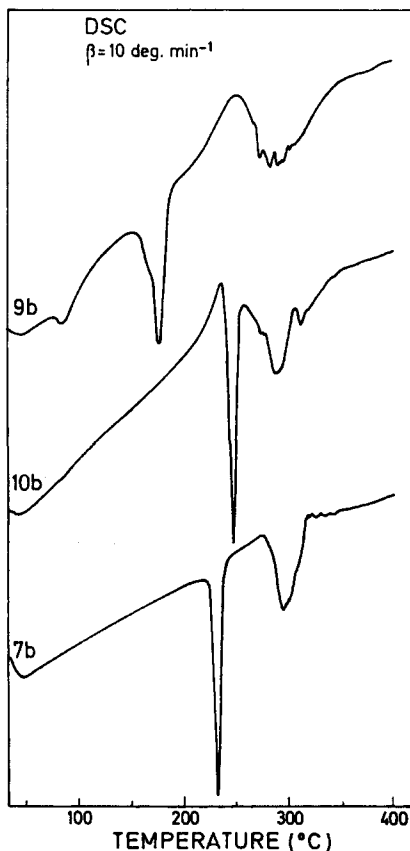


Fig. 3 DSC curves of compounds 7b, 9b and 10b (heating rate=10°C min⁻¹)

Table 6 Thermal data of tropane-6-spiro5'-hydantoin derivatives (Compounds 9b, 10b and 7b)

Compound	M.W.	DSC entothermal effect		$T_m/^{\circ}\text{C}$	$-\Delta H/\text{J g}^{-1}$	$-\Delta H/\text{KJ mol}^{-1}$
		$T_o/^{\circ}\text{C}$	$T_b/^{\circ}\text{C}$			
9b	237	164	173	172	56.1	13.29
		(437)	(446)	(445)		
10b	237	237	245	240	44	10.43
		(510)	(518)	(513)		
7b	295	221	228	219	56.6	16.69
		(494)	(501)	(492)		

Notes: T_o = extrapolated onset temperature; T_b = bottom peak temperature; T_m = estimated melting point temperature from open capillary method (Büchi immersion apparatus). Values between parenthesis are reported in K. M.W. = Molecular Weight

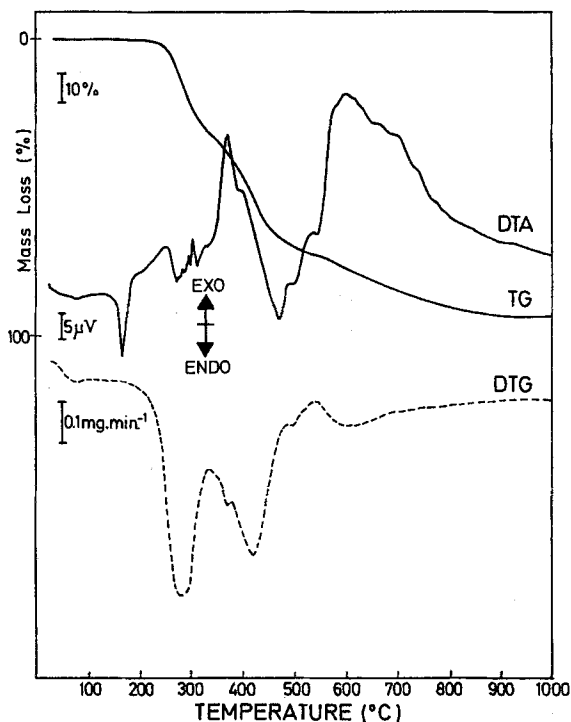


Fig. 4 DTA-TG-DTG curves of compound 9b (hydantoin ring in position β) obtained in nitrogen (heating rate = $10^{\circ}\text{C min}^{-1}$)

enthalpy. It was explained by taking into account the presence of this additional $-\text{O}-\text{CH}_2-\text{CH}_2-\text{O}-$ substituent in the ring. It can also be seen that melting temperatures estimated using a Büchi immersion apparatus were of the same order

as the extrapolated onset temperatures, except for sample 9b, because of the more complex DSC shape, which makes extrapolation more difficult. However, compound 9b exhibits a weak endothermic peak at lower temperature than 10b, possibly associated with the elimination of solvents occluded in the crystals which were used for purification and recrystallization.

According to DSC results, it seems that tropane-6-spiro-5'-hydantoin derivatives with hydantoin ring in β position (i.e., as found in compounds 9b and 7b), are thermally less stable than those in α position (sample 10b). In this sense, it has been found previously [15, 16] that isomers with α configuration at the spiro atom C_3 , as shown Scheme 2, showed higher melting temperatures (open capillary tube) in the range 300–380°C.

Figures 4 and 5 show the DTA-TG-DTG curves obtained for isomers 9b and 10b in nitrogen flow. Heating of sample 9b leads first to the elimination of occluded solvents entrapped in the crystals. An important thermal event is observed when the sample melts at 171°C with extrapolated onset temperature at 157°C. These results agree with DSC curves shown in Fig. 3. Above 250°C, a degradation process starts. On further heating, as the temperature reaches 340°C, a mass loss of 22% is observed, with an intense DTG peak centered at 280°C and

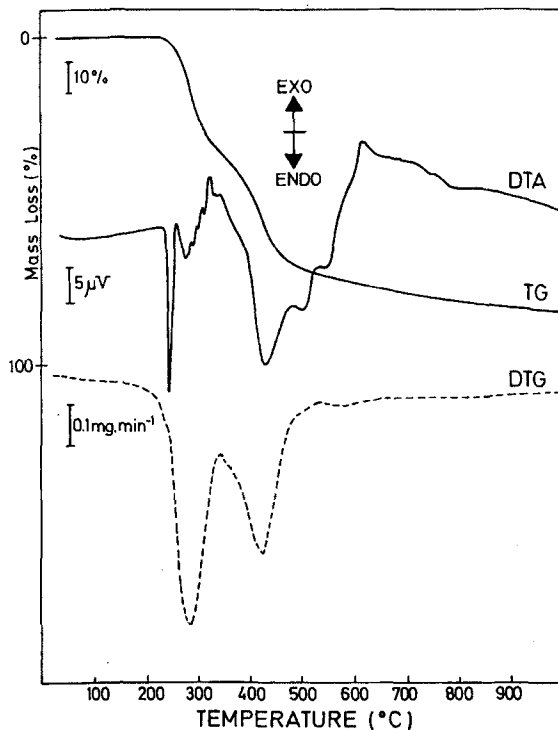


Fig. 5 DTA-TG-DTG curves of compound 10b (hydantoin ring in position α) obtained in nitrogen (heating rate=10°C min⁻¹)

several weak endothermal DTA effects. Upon further heating, a more completed degradation of the sample is observed, as indicated by an exothermal DTA effect centered at 370°C followed by an endothermal effect centered at 480°C. A second important mass loss calculated as high as 42% is produced at 540°C with a DTG peak at 420°C and an intermediate DTG peak detected at 370°C as a shoulder. Upon further heating, the sample undergoes a final degradation process, producing a carbonaceous residue after heating at 1000°C. The total mass loss after complete pyrolysis was calculated to be as high as 89%.

Sample 10b exhibits an endothermal DTA effect at 245°C with extrapolated onset temperature of 239°C, being in accordance with DSC data (Fig. 3), which is associated with the melting of this tropane-6-spiro-5'-hydantoin derivative containing the hydantoin ring is α position. At the same time, a degradation process is taking place when the sample undergoes the solid-liquid transition, which produces also weak endothermal DTA effects and an important mass loss calculated as 32% after heating at 340°C. The DTG curve shows an intense peak at 281°C, in connection with the above mentioned degradation process. Further heating produces several broad endothermal DTA peaks at 440, 500 and 545°C, associated with degradation and pyrolysis with decomposition of the heated products, producing a mass loss of 32% after heating from 340° up to 520°C, and a single and intense DTG peak at 423°C. The total mass loss after heating at 1000°C was calculated to be as high as 75%.

Degradation of hydantoin and tropane rings with molecular breakdown and cracking of the alkyl chain are probably two features produced after thermolysis of these compounds containing the tropane-6-spiro-5'-hydantoin structure. The degradation processes that are taking place after heating these compounds in nitrogen are not yet clear and they are studied by IR and mass spectroscopies for a complete interpretation. Derivative 9b shows a lower thermal stability than its isomer 10b, owing to structural reasons because the former has a β configuration of the hydantoin ring, while the latter has an α configuration, as discussed in connection with DSC results. However, according to DTG results, as shown in Figs 4 and 5, degradation processes above the solid-liquid transition seem to be essentially the same, being the subject of further research.

* * *

One of the authors (Dr. M.V.) thanks partial financial support from CICYT through research project PA 86-0317. Thanks are extended to Ms. A. García and Mr. J. C. Rivero for artwork.

References

- 1 J. L. Ford and M. H. Rubinstein, *J. Pharm. Pharmacol.*, 29 (1977) 209.
- 2 M. P. Summers, *J. Pharm. Sci.*, 67 (1978) 1606.
- 3 E. Nauchbaur, E. Baumgartner and J. Schober, *Proc. 2nd European Symposium on Thermal Analysis*, D. Dollimore, Ed., Heyden, London 1981, p. 417.

- 4 M. Kamimoto, R. Sakamoto, Y. Takahashi, K. Kanari and T. Ozawa, *Thermochim. Acta*, 74 (1984) 281.
- 5 A. M. Wynne, *J. Chem. Educ.*, 64 (1987) 180.
- 6 L. Stradella and M. Argentero, *Thermochim. Acta*, 219 (1993) 315.
- 7 R. Chandra and N. N. Ghosh, *Thermochim. Acta*, 189 (1991) 83.
- 8 P. Hanisch, A. J. Jones, A. F. Casey and J. E. Coates, *J. Chem. Soc. Perkin Trans.*, 2 (1977) 1202.
- 9 F. W. Vierhapper and E. L. Eliel, *J. Org. Chem.*, 44 (1979) 1081.
- 10 G. G. Trigo, M. Martínez and E. Gálvez, *J. Pharm. Sci.*, 70 (1981) 87.
- 11 G. H. Dewar, R. T. Parfitt and L. Sheh, *Eur. J. Med. Chem.*, 20 (1985) 228.
- 12 S. Viudas, F. Sanz, A. García and M. Illera, *Arch. Farmacol. Toxicol.*, 4 (1978) 3.
- 13 M. P. Díaz, N. Romera, J. M. Vivas, M. Rebuelta, M. J. Lázaro-Carrasco, M. Martínez and J. González, *Anal. Real Acad. Farm.*, 53 (1987) 579.
- 14 G. G. Trigo and M. Martínez, *Pharm. Mediterranea*, 10 (1974) 643.
- 15 M. Villacampa, Ph. D. Thesis, Universidad Complutense, Madrid 1990.
- 16 M. Villacampa, M. Martínez, G. González-Trigo and M. M. Solhüber, *J. Heterocyclic Chem.*, 29 (1992) 1541.
- 17 M. Villacampa, M. Martínez, G. González-Trigo and M. M. Solhüber, *Heterocycles*, 34 (1992) 1885.
- 18 T. A. Montzka and J. D. Matiskella, *J. Med. Chem.*, 20 (1977) 453.
- 19 T. V. Lee, in *Comprehensive Organic Synthesis* (B. M. Trost and I. Fleming, general editors), Vol. I, Pergamon Press, NY, 1991, p. 251.
- 20 R. I. W. Cremllyn and M. Chisholm, *J. Chem. Soc. C*, (1967) 1762.
- 21 G. G. Trigo, C. Avendano, E. Santos, J. T. Edward and S. C. Wong, *Can. J. Chem.*, 57 (1979) 1456.
- 22 H. S. Tager and H. N. Christensen, *J. Am. Chem. Soc.*, 94 (1972) 968.